



# A synthesis dataset of permafrost-affected soil thermal conditions for Alaska, USA

Kang Wang<sup>1</sup>, Elchin Jafarov<sup>2</sup>, Kevin Schaefer<sup>3</sup>, Irina Overeem<sup>1</sup>, Vladimir Romanovsky<sup>4</sup>, Gary Clow<sup>1,5</sup>, Frank Urban<sup>5</sup>, William Cable<sup>4,9</sup>, Mark Piper<sup>1</sup>, Christopher Schwalm<sup>6</sup>, Tingjun Zhang<sup>7</sup>, Alexander Kholodov<sup>4</sup>, Pamela Sousanes<sup>8</sup>, Michael Loso<sup>8</sup>, and Kenneth Hill<sup>8</sup>

<sup>1</sup>CSDMS, Institute of Arctic and Alpine Research, University of Colorado, Boulder, CO 80309, USA

<sup>2</sup>Los Alamos National Laboratory, Los Alamos, New Mexico, 87545, USA

<sup>3</sup>National Snow and Ice Data Center, Cooperative Institute for Research in Environmental Sciences, University of Colorado Boulder, Boulder, CO 80309, USA

<sup>4</sup>Geophysical Institute Permafrost Laboratory, University of Alaska, Fairbanks, AK 99775, USA

<sup>5</sup>U.S. Geological Survey, Lakewood, CO 80225, USA

<sup>6</sup>Woods Hole Research Center, Falmouth MA 02540, USA

<sup>7</sup>MOE Key Laboratory of Western China's Environmental Systems, College of Earth and Environmental Sciences, Lanzhou University, Lanzhou 730000, China

<sup>8</sup>National Park Service Arctic Central Alaska Inventory and Monitoring Networks Fairbanks, AK 99709

<sup>9</sup>Alfred Wegener Institute Helmholtz Center for Polar and Marine Research, 14473 Potsdam, Germany

**Correspondence:** Kang Wang (Kang.Wang@colorado.edu)

**Abstract.** Recent observations of near-surface soil temperatures over the circumpolar Arctic show accelerated warming of permafrost-affected soils. A comprehensive near-surface permafrost temperature dataset is critical to better understand climate impacts and to constrain permafrost thermal conditions and spatial distribution in land system models. We compiled a soil temperatures dataset from 72 monitoring stations in Alaska using data collected by the U.S. Geological Survey, the National Park Service, and the University of Alaska-Fairbanks permafrost monitoring networks. The array of monitoring stations spans a large range of latitudes from 60.9°N to 71.3°N and elevations from near sea level to 1327 m, comprising tundra and boreal forest regions. This dataset consists of monthly ground temperatures at depth up to 1 m, volumetric soil water content, snow depth, and air temperature during 1997 - 2016. Due to the remoteness and harsh conditions, many stations have missing data. Overall, this dataset consists of 41,667 monthly values. These data have been quality controlled in collection and processing. Meanwhile, we implemented data harmonization validation for the processed dataset. The final product (PF-AK, v0.1) is available at the Arctic Data Center (<https://doi.org/10.18739/A2KG55>).

## 1 Introduction

Permafrost is frozen ground that remains at or below 0 °C for at least two consecutive years and may be found within about a quarter of the terrestrial land area in the Northern Hemisphere and 80% of the land area in Alaska (Brown et al., 1998; Zhang et al., 1999; Jorgenson et al., 2008). Continuous warming of the near-surface air temperatures over the Alaskan Arctic (Romanovsky et al., 2015; Wang et al., 2017) causes warming and thawing of permafrost in Alaska, which is expected to



continue throughout the 21st century with multi-billion dollar impacts on infrastructure and ecosystems (Callaghan et al., 2011; Hinzman et al., 2013; Liljedahl et al., 2016; Shiklomanov et al., 2017; Melvin et al., 2017). Permafrost thaw may have global consequences due to the potential for a significant positive climate feedback related to newly released carbon previously stored within the permafrost (Abbott et al., 2016; Schaefer et al., 2014; Knoblauch et al., 2018). Modeling studies 5 indicate that greenhouse gas emissions following thaw would amplify current rates of atmospheric warming (McGuire et al., 2016). However, large uncertainties exist regarding the timing and magnitude of this permafrost-carbon feedback, in part due to challenges associated with representation of permafrost processes in the climate models and the lack of comprehensive permafrost datasets with which to test such models (Koven et al., 2015; McGuire et al., 2016). There is an immediate need 10 for ready-to-use reliable near-surface permafrost datasets, including ground temperatures, soil moisture, and related climatic factors (such as air temperature and snow depth), which can serve as benchmarks for the modeling community and help to evaluate potential physical, societal, and economic impacts.

The permafrost extent map by Brown et al. (1998) is one of the most frequently and widely used metrics for comparing permafrost model results against real-world data (Koven et al., 2015; McGuire et al., 2016). Another widely used permafrost dataset is the Russian Soil Temperature dataset of daily ground temperature measurements at different depths ranging from 0 15 to 3.2 m for 51 years (Sherstiukov, 2012). An additional ground temperature dataset includes daily-mean ground temperatures at various depths from 0 to 3.2 m at more than 800 stations in China which in selected locations dates back to the 1950s (Wang et al., 2015).

A typical permafrost monitoring station consists of an air temperature sensor, a snow depth sensor, soil moisture sensors, and soil temperature sensors. In-situ observations of ground temperatures from the Alaskan Arctic region have been dispersed 20 over different monitoring efforts, which are spread over varying timespans, and have non-uniform depths. The maximum depth of a typical monitoring station ranges from 1 to 3 m below the ground surface. However, not all stations use this design. For example, the National Park Service of Alaska network does not collect soil moisture data. Also, data from permafrost monitoring stations in Alaska are not archived in a common standardized format and are hosted by different academic and government agencies, such as the Arctic Data Center, the Global Terrestrial Network for Permafrost (GTN-P), the Long Term 25 Ecological Research Network (LTER), and the U.S. Geological Survey (USGS). Thus, we compiled a ready-to-use permafrost dataset in order to allow for efficient data retrieval and processing for permafrost-related analysis.

We compiled a first integrated near-subsurface ground temperatures dataset for permafrost-affected soils across Alaska from the three most reliable sources monitoring networks over several past decades: the Geophysical Institute Permafrost Laboratory at the University of Alaska Fairbanks (GI-UAF), National Park Services in Alaska (NPS), and the USGS. This 30 synthesis permafrost dataset for Alaska (PF-AK, version 0.1) includes measured air and ground temperatures, snow depth and soil volumetric water content for 72 permafrost monitoring stations across the state of Alaska. We provide detailed information and meta-data on the compiled dataset so that potential users can have a full understanding of the data and its associated limitations. Furthermore, we implemented two types of data harmonization validation: (i) we test for inconsistencies between air and ground temperature trends; and (ii) we use the snow heat transfer metric to validate the relations between seasonal



temperature amplitudes and snow depth. These technical validation would be useful for proving data harmonization and reusing these data.

## 2 Data sources and processing

### 2.1 Permafrost monitoring networks

5 Our synthesis permafrost dataset for Alaska is based on observed in-situ data collected by the USGS, NPS, and GI-UAF teams. In addition to these permafrost monitoring networks in Alaska, there is the Circumpolar Active Layer Monitoring (CALM) monitoring network measuring active layer thickness (ALT) - the maximum soil depth above permafrost that thaws every summer and refreezes in the winter. ALT is measured by physical probing on grids ranging in size of  $100 \times 100$  to  $1000 \times 1000$  meters, along specified transects, or from permanently installed frost tubes (Shiklomanov et al., 2008). Here we do not include  
10 CALM data, since this particular data is already well organized, well documented, easily accessible, and does not require any significant data processing (Brown et al., 2000; Shiklomanov et al., 2008).

In the late 1990s, researchers at the GI-UAF established a near-surface permafrost monitoring system consisting of 27 stations across Alaska, primarily along the Trans-Alaskan highway (triangles in Fig.1)(Romanovsky et al., 2015). Similarly, the USGS installed permafrost stations to monitor permafrost conditions within the two federally managed areas on the North  
15 Slope, the National Petroleum Reserve-Alaska and the Arctic National Wildlife Refuge. Since August 1998, the USGS has served 17 automated stations in the area spanning latitudes from  $68.5^{\circ}\text{N}$  to  $70.5^{\circ}\text{N}$  and longitudes from  $142.5^{\circ}\text{W}$  to  $161^{\circ}\text{W}$  (stars in Fig.1) (Urban and Clow, 2017). NPS has monitored permafrost conditions since 2004 (Hill and Sousanes, 2015). All monitoring stations are installed on undisturbed land (Fig.2) at a minimum specified distance from nearby infrastructure. This protocol for installation ensures no biases associated with anthropogenic or ecosystem disturbances, which is one of the main  
20 differences with traditional meteorological stations which are often associated with airstrips and villages in Alaska. All the permafrost networks utilize radiation-shielded thermistors (Campbell Scientific CSI 107 temperature probes) to monitor air temperature. In the GI-UAF and NPS network, the air temperature sensors were installed at 1.5 or 2.0 m above the ground surface, whereas the USGS network monitors air temperature at 3.0 m above the ground surface in order to minimize damage by wildlife. Despite the installation of air temperature sensors at different heights, the measurements of air temperature are  
25 considered comparable on a monthly scale assuming efficient mixing of the near-surface atmosphere.

To monitor near-surface ground temperature, the networks use either a probe with several thermistors embedded into a single rod, typically 1.0 to 1.5 m long, or several individual Campbell Scientific 107 thermistors anchored at specified depths within a single hole. The thermistor temperature sensors are designed to record temperatures ranging from  $-30$  to  $75^{\circ}\text{C}$ ; the 107 sensors record temperatures from  $-35$  to  $50^{\circ}\text{C}$ . An ice-bath calibration is a required procedure before installation of these  
30 probes. The ice-bath calibration includes placing the sensors into an insulated container filled with a mixture of ice shavings and distilled water, measuring the temperature, and recording the offset from  $0^{\circ}\text{C}$ . This measured offset is then used to correct the temperature measurements. The average accuracy of these sensors is  $\pm 0.01^{\circ}\text{C}$  (Romanovsky et al., 2008). For the USGS network, the thermistor sensors are installed inside a tight-fitting fluid-filled 125-cm-long plastic tube to measure ground

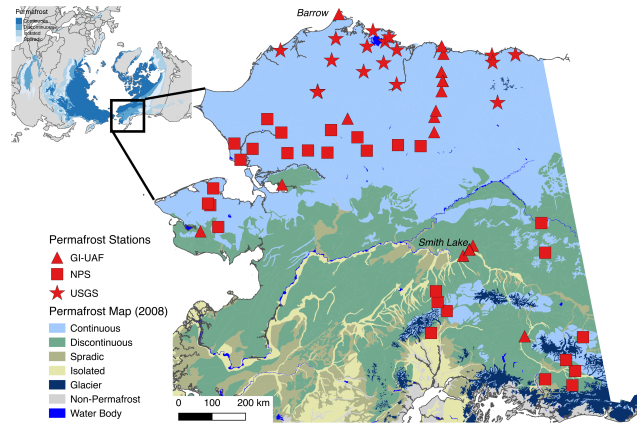


**Figure 1.** Locations of Geophysical Institute-University of Alaska Fairbanks (GI-UAF), U. S. Geological Survey (USGS), and National Park Services (NPS) permafrost monitoring stations in Alaska. The basemap is a new permafrost distribution of Alaska compiled by Jorgenson et al. (2008).

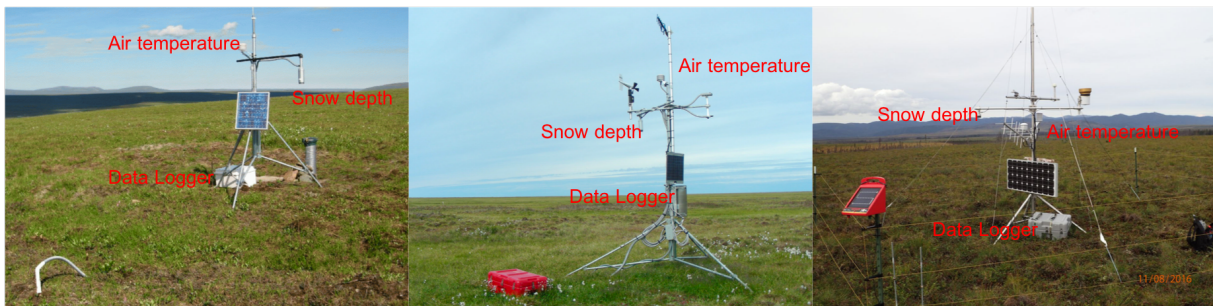


**Figure 2.** Typical permafrost observing stations. Left is Imnaviat 1 site ( $68.64^{\circ}\text{N}$ ,  $149.35^{\circ}\text{W}$ ) in the GI UAF network (source: <http://permafrost.gi.alaska.edu/site/im1>); middle is the Drew Point station ( $70.86^{\circ}\text{N}$ ,  $153.91^{\circ}\text{W}$ ) in the USGS network (source: <http://pubs.usgs.gov/ds/0977/DrewPoint/DrewPoint.html>); right is the Wigand site ( $63.81^{\circ}\text{N}$ ,  $150.109^{\circ}\text{W}$ ) in the NPS network.

temperatures at 5, 10, 15, 20, 25, 30, 45, 70, 95, and 120-cm depth (Urban and Clow, 2017). The NPS has three to four soil temperature sensors (CS1-107) installed in individual holes at 10, 20 and 50 cm depths, and at several locations an additional sensor at 100 cm. The ground-measurement depths vary station by station within the GI-UAF network, typically ranging from the ground surface (i.e., 0 m) to 1 m below the ground surface. It is important to note that most of the installed probes frost heave with time, and heaving depths are adjusted accordingly by subtracting the heaving values yearly. The released data account for the heave and have corrected ground temperatures.

Both the USGS and the GI-UAF networks measure liquid soil moisture using a Hydra Probe sensor developed by Stevens Water Monitoring Systems Inc. The Stevens Hydra Probe has a reported accuracy of  $\pm 0.03 \text{ m}^3/\text{m}^3$  (Bellingham, 2015). Each volumetric water content sensor was calibrated in accordance with the soil texture in laboratory while uncertainties associated with the sensor's sensitivity still exist under specific conditions, e.g., for peat. The measured liquid soil moisture from a Hydro



Probe cannot be directly compared with the total soil moisture content values produced by land system models because in most of the models, soil moisture includes both ice and liquid water, where HydroProbe measures only liquid soil moisture. The USGS network measures soil moisture at one depth, approximately 0.15 m below the ground surface in all cases. The soil moisture sensors depths vary between stations for the GI-UAF network because they are installed at depths depending 5 on the soil profile and texture within the active layer. The GI-UAF network measures soil moisture typically at three different depths within the active layer, ranging from 0.10 to 0.60 m. The NPS network does not include moisture probes at any of their monitoring stations. Our processed dataset presents only the upper layer (up to 0.25 m) soil water content.

Snow depth is measured once per hour with a SR50 or SR50A ultrasonic distance sensor (Campbell Sci. Inc.) at all of the stations. This downward-looking sensor is mounted on a cross-arm typically at 2.5 m above the ground surface for the USGS 10 and NPS networks, and 1.5 m above the ground surface for the GI-UAF network respectively. The factory evaluated accuracy is  $\pm 0.01$  m or 0.4% of the distance to the ground surface. It's important to note that vegetation at the ground surface might influence shallow snow-depth measurements.

## 2.2 Data processing workflow

All three networks apply data processing and quality-control (QC) checks before release. Typically, quality control occurs 15 shortly after annual summer field campaigns; the fully-processed and QC-ed data become publicly available a year after the data collection. In the present version of the permafrost dataset, we use USGS Data Series 1021, which includes data through July 2015 (URL: <https://pubs.er.usgs.gov/publication/ds1021>). The GI-UAF and NPS data were collected and processed by December, 20, 2017, and latest calibrated data was August, 2016. The GI-UAF data are available on [http://permafrost.gi.alaska.edu/sites\\_map](http://permafrost.gi.alaska.edu/sites_map). NPS data is available from <https://irma.nps.gov/DataStore/Reference/Profile/2240059> and <https://irma.nps.gov/DataStore/Reference/Profile/2239061>.

Fig.3 shows a schematic representation of the data processing workflow used to compile the near-surface permafrost dataset. To standardize the ground temperature depth in the benchmarking dataset, we linearly interpolate ground temperatures for target depths: 0.25, 0.50, 0.75, and 1.00 m; however, we did not extrapolate beyond the deepest observed depth at any site. The USGS and NPS network releases data at hourly resolution, whereas the GI-UAF network releases data at daily resolution. 25 Since the most common model data output intervals of the land system and global climate models are monthly, we calculate monthly means of all measurements, including air and ground temperatures, snow depth, and soil water content. In addition to monthly data, we calculate annual means to allow evaluation of long-term trends between ambient and ground temperatures. Thus, the dataset also provides annual statistics including mean-annual air temperature (MAAT); mean-annual ground surface temperature (MAGST); mean-annual ground temperature at 1 m (MAGT at 1 m); mean and maximum seasonal snow depth 30 (SND); and maximum, mean, and minimum soil volumetric water content (VWC). We also calculated the Frost Number (i.e., Eq.1-3) for air temperature and ground temperatures following Nelson and Outcalt (1987). The Frost Number serves as a simplified index for the likelihood of permafrost occurrence.

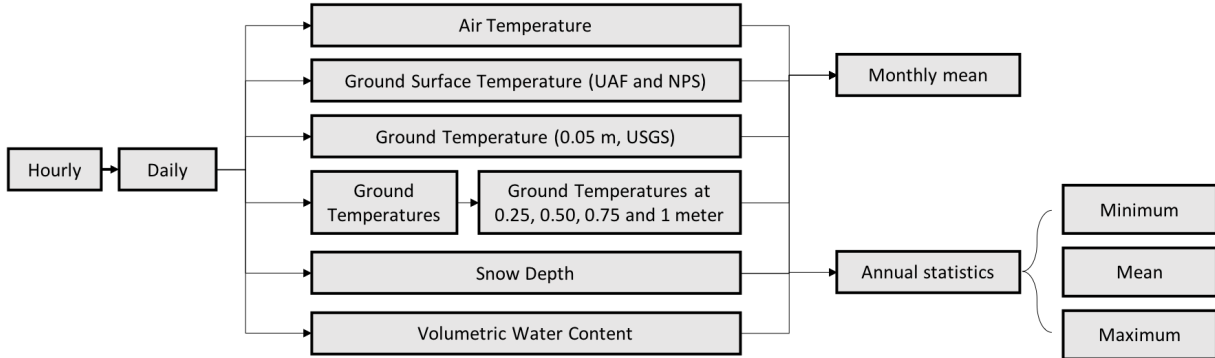


**Figure 3.** Schematic representation of the data processing workflow used to compile the permafrost dataset in the Alaska.

$$FrostNumber = \frac{\sqrt{DDF}}{\sqrt{DDF} + \sqrt{DDT}} \quad (1)$$

$DDT$  and  $DDF$  are given by

$$DDT = \int T(t)dt, T(t) > 0^\circ C \quad (2)$$

and

$$DDF = \int |T(t)|dt, T(t) \leq 0^\circ C \quad (3)$$

Data from many sites have gaps and discontinuities due to harsh environmental conditions and wildlife that may interrupt the monitoring. There are various methods for calculating monthly means from incomplete time series data. For example, the USGS standards allow only 5% of missing values for both monthly and annual mean temperature data (Urban and Clow, 2017). The World Meteorological Organization (WMO) does not allow gaps of more than three consecutive days or more than 5 days total from each monthly data series (Plummer et al., 2003). Other researchers are more tolerant of missing data, acknowledging the difficulty of data collection in remote cold regions. Menne et al. (2009) allows up to 10 missing days in a monthly time series. Bieniek et al. (2014) calculated monthly averages using at least 15 days. Here we calculated monthly means for any station which has at least 20 days of measurements for that specific month. The annual means were calculated from daily data. Due to the scarcity of the data, we calculate the annual means only for those years with a coverage of at least 90% of the daily data. For this reason, we present annual means for air and ground temperatures as well as soil moisture, derived from daily data.

During the dataset compilation, we identified similarly named sites with different installation times and locations that do not match precisely. It is important to note that these sites, even when located nearby each other, may have considerably different environmental conditions, and thus, different ground temperature thermodynamics. Our dataset allows only one name per



station site. We identified two overlapping sites in our new synthesis dataset: the Deadhorse site maintained by GI-UAF, and the Awuna site maintained by USGS. Both sites have new monitoring stations, and the old ones have been decommissioned. The environmental conditions for the newer Deadhorse station remained the same assuring data consistency. However, the environmental conditions between two monitoring stations at the Awuna site are quite different: the original Awuna site was 5 located on a ridge, whereas the new site is in a valley 1.9 km away. Nevertheless, the temperature data are consistent between the old and new station at the Awuna site. The old site (Awuna1) did not monitor soil moisture, which would be expected to be more site-specific and spatially variable. Thus, in this dataset, we present both the new and old sites' records.

### 2.3 Validation of data harmonization

Despite the fact that individual station observations had originally been quality-controlled, we still need to examine our own 10 results of the data harmonization. Here we implemented two ways of validation, the first way compares the trends in air and ground temperatures; and the second method examines the effects of snow on ground thermal states.

The primary objective of the trend analysis was to evaluate the consistency between trends at each station (for different depths) and between stations rather than inform inter-annual variability. Most of the estimated trends have a short observational period (see Tab.1). We chose to show trends only for those stations with more than five available annual means. Currently, some 15 of the time series are too short to provide significant trends. As more data becomes available in the future, a more rigorous analysis will be possible. It is well known that climatic trend analysis requires more than 30 years of time series (IPCC, 2013). On the other hand, Box et al. (2005) showed that 15 years are sufficient for inter-annual variability diagnosis to be statistically significant. Since the time series for most of the stations do not exceed 15 years we calculate trends for temperatures at different depths to determine inconsistencies between air and ground temperature trends in terms of sign's differences.

20 The second aspect is to examine the physical mechanism among air temperature, snow cover and ground thermal states, which is an auxiliary validation of the dataset. Seasonal snow cover will keep the ground warm by reducing the direct impact of cold air temperature during the winter (Yershov and Williams, 2004). Considering a semi-infinite column, the damping of the ground temperature annual cycle is depending on snow depth and thermal properties. In this study, the snow period was defined as October through March. To complement the snow thermal metric introduced by Slater et al. (2017) for Alaska, we 25 calculated the effective snow depth measurements ( $SND_{eff}$ ) over the period from October through March. The temperature amplitudes of air ( $Amp_{air}$ ) and ground surface ( $Amp_{gnd}$ ) temperatures were calculated following Slater et al. (2017), which is calculated only for stations with available snow depth data. The snow and heat transfer metric (SHTM) was featured as the normalized temperature amplitude difference ( $\Delta Amp_{norm}$ ) (i.e., Eq.4-6):

$$\Delta Amp_{norm} = \frac{Amp_{air} - Amp_{gnd}}{Amp_{air}} \quad (4)$$

30  $Amp_{air}$  and  $Amp_{gnd}$  are given by

$$Amp_{air} = \frac{1}{2} [Max(T_{air}) - Min(T_{air})] \quad (5)$$



and

$$Amp_{gnd} = \frac{1}{2} [Max(T_{gnd}) - Min(T_{gnd})] \quad (6)$$

### 3 Results

#### 3.1 Overview of this dataset

5 Tab.2 presents an overview of the data compiled in the permafrost benchmarking database for Alaska. Our dataset consists of a total of 41,667 monthly data values. The VWC shown in Tab.2 is from the upper part of the soil (i.e., up to 25 cm depth). The VWC measurements are mainly available on the North Slope of Alaska. Maximum VWC is more important for understanding active layer dynamics, especially during summer. Notably, the maximum VWC has a three times larger spatial variance than the annual means. Three sites, Chandalar Shelf, Pilgrim Hot Springs, and Red Sheep Creek, were much wetter than other sites  
10 (maximum VWCs exceeding  $0.7 \text{ m}^3/\text{m}^3$ ). This is mainly because these sites are close to a water body.

Snow depth is spatially complex over Alaska, although with a general trend of increasing snow depth in the southern part of the state, according to the synthesis dataset (Fig.4). In the Alaskan Arctic, snow cover is shallower than in the southeast region. The highest maximum seasonal snow depth was 1.5 m at the Gates Glacier station (which is not actually located on the glacier) in Wrangell-St. Elias National Park. The lowest maximum snow depth occurs at WestDock near the Beaufort Sea in  
15 Prudhoe Bay at only 0.09 m in 2010 (note that, there were available snow depth measurements only for 2010, i.e., we did not have enough data for any other years). Other two sites, Asik in Noatak National Park and Serpentine in Bering Land Bridge National Preserve, also showed a shallow snow cover in recent years (We don't intend to explain the reasons much more while they are mainly because of the topographical cause, e.g., Asik is a site on an exposed ridge).

In this dataset, we derived the frost number index for air and ground temperatures at various depths (Fig.5 and Tab.3).  
20 Because many stations do not have sensors at depth  $> 1 \text{ m}$ , we report the freezing/thawing indices of air, ground surface, and 0.5 m below the ground surface in Fig.5, with all available results listed in Tab.3. Overall, almost all stations have air frost number above 0.5. Stations on the North Slope have both air and ground surface frost numbers exceeding 0.6. In interior and southern Alaska, air frost numbers were above 0.5, although the ground surface frost numbers were much lower due to the thicker snow cover in this region. In the Alaskan Arctic, thawing indices at ground surface were generally lower than air  
25 according to the station observations. There were 13 stations with a zero thawing index of ground temperature at 0.5 m. These results indicate a shallow active layer ( $< 0.5 \text{ m}$ ) at these sites, which is consistent with the Active Layer Monitoring Network CALM data. Another five stations have a thawing index of ground temperature at 0.5 m less than  $10 \text{ }^{\circ}\text{C}$ -days. The calculated frost number indices are consistent with the existing permafrost distribution map over the Alaska (Jorgenson et al., 2008).

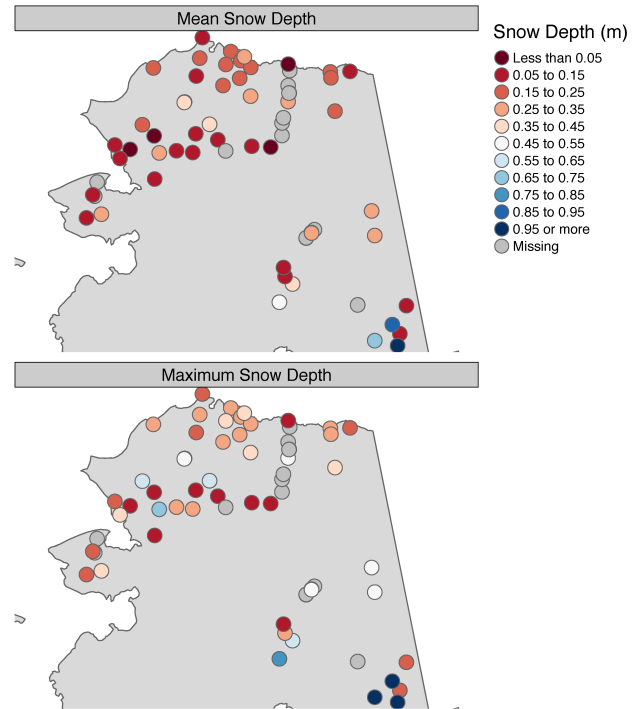


**Figure 4.** Overview of spatial distribution of snow depth, including annual mean snow depth and maximum snow depth.

### 3.2 Validation of data harmonization

We examined the consistency among the trends of MAAT, MAGST, and MAGT at 1 m depth. Typically, if MAAT has a long-term positive trend then MAGST is expected to have a positive trend, even if the rate is damped (Romanovsky et al., 2015). Similarly, signs of trends in MAGST and MAGT at 1 m depth, and MAAT and MAGT at 1 m depth are hypothesized to be consistent (Romanovsky et al., 2015). Here we show the annual mean temperatures at four stations, Drew Point, Fish Creek, Niguanak, and Tunalik, with ten or more years of data (Fig.6). Mean annual air, ground surface, and ground temperature at 1 m indicates consistent warming at rates of 0.07 – 0.18, 0.14 – 0.23, and 0.12-0.22 °C/year, respectively. An obvious feature was that at Fish Creek, ground surface temperature and ground temperature at 1 m showed amplified warming rates compared to the magnitude of the air temperature increases, which can be explained by the significant increase of seasonal snow depth during the same period. Seven sites (Smith Lake 3, Ivotuk 4, GGLA2, Galbraith Lake, CTUA2, CREA2, and Chandalar Shelf) show inconsistent trends (Fig.7). However, when we considered the trend estimate uncertainties, we found that only two stations (Chandalar Shelf and Galbraith Lake) have significantly opposing trends between air temperature and ground surface temperature. Annual variation in snow depth may be responsible for the sign inconsistency between trends at these sites, but we lack observational evidence for this because snow depth data are not collected here.

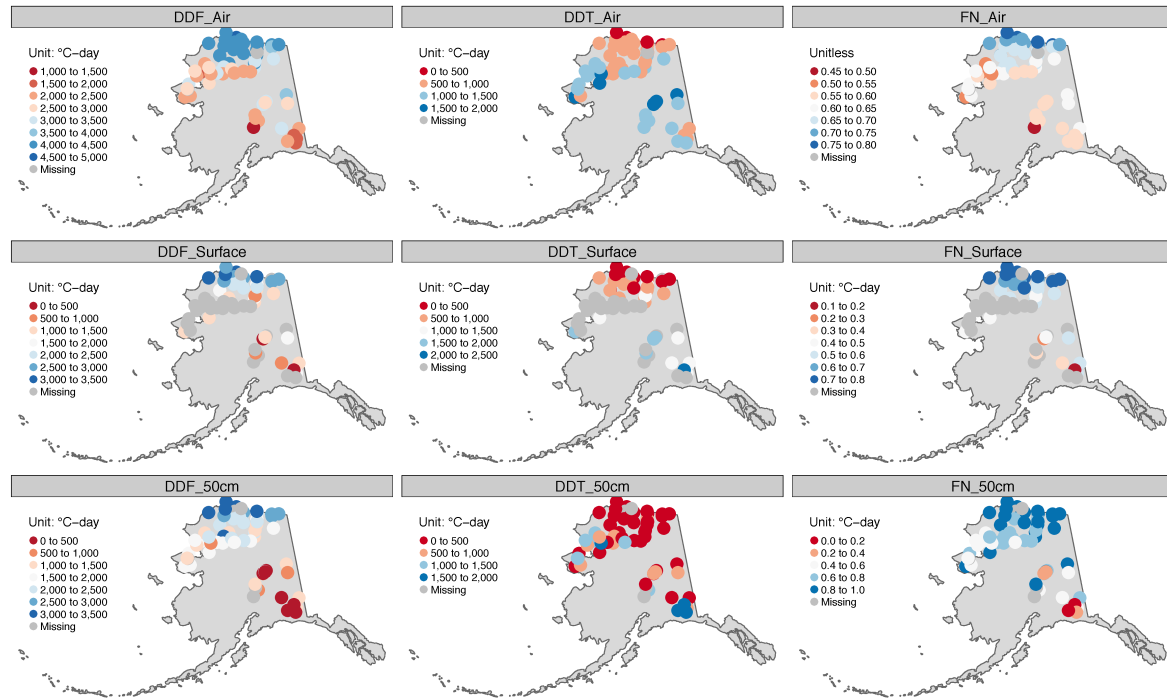


**Figure 5.** Overview of spatial distribution of freezing/thawing index from air, ground surface temperature, and ground temperature at 0.50 m. Frost Number (FN) was derived from the freezing/thawing index according to Nelson and Outcalt (1987).

Besides, there are several sites in a small area while indicated inconsistency in air temperature trends. This mainly because of different observational periods and relatively short duration of records. Typically, there are several Smith Lake (SL) permafrost monitoring stations which are located north of the UAF campus and west of Smith Lake with varying environmental conditions. (SL1 is in a White Spruce forest with high canopy; SL2 is in a dense diminutive Black Spruce forest; and SL3 is located at the edge of the forest surrounded by Black Spruce trees and tussock-shrubs; and SL4 is characterized by hummocks of sedges (tussocks) and shrubby vegetation with sparse Black Spruce.) The environmental conditions at SL3 site provide favorable conditions for permafrost existence. The SL3 site has the longest air temperature record indicating a cooling trend over the observational period (Fig.8A). After calculating the differences between measured data for all three sites we applied corresponding corrections and extend the data at all three sites. The overlap period (2006-2012) showed a consistent variation with the roughly constant offset between Smith Lake 2 and Smith Lake 3. By using the offset, we extended the records at Smith Lake 3 to 2015. Fig.8B shows that extending the time series reduces the trend magnitude and changes the negative sign in SL3 trend to positive, indicating the important difference between a complete versus a sparse time series.

Finally, we examined the physical relations among air temperature, snow cover and ground thermal states. We used the SHTM to examine the relationship between the effective snow depth and normalized temperature amplitude difference ( $\Delta Amp_{norm}$ ) across the entire in-situ dataset. It should be noted that we lack sufficient observations (i.e., sites with snow, air temperature and

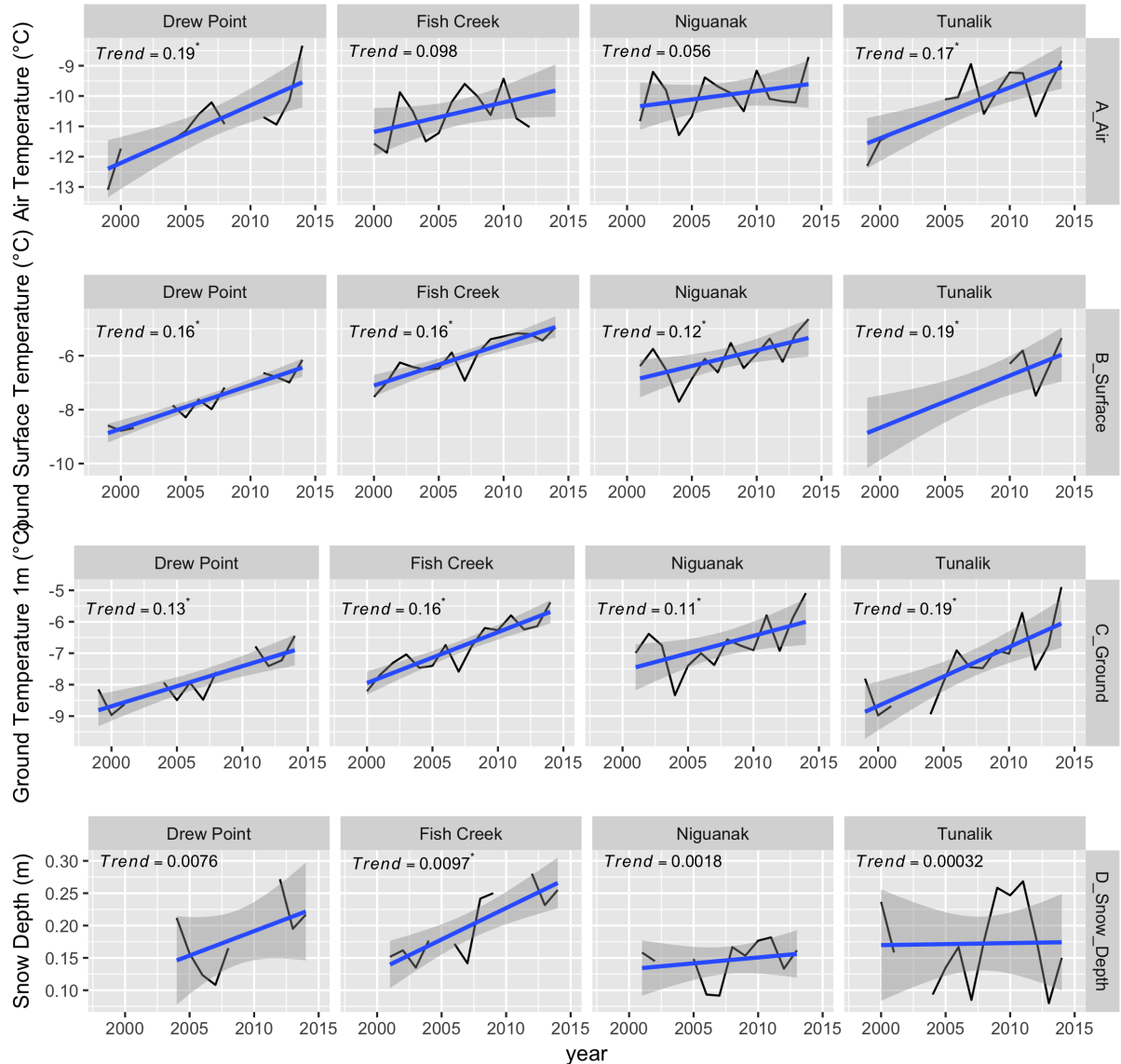


**Figure 6.** Examples of time-series in mean annual air, ground surface, ground temperature at 1 m below ground surface, and snow depth.

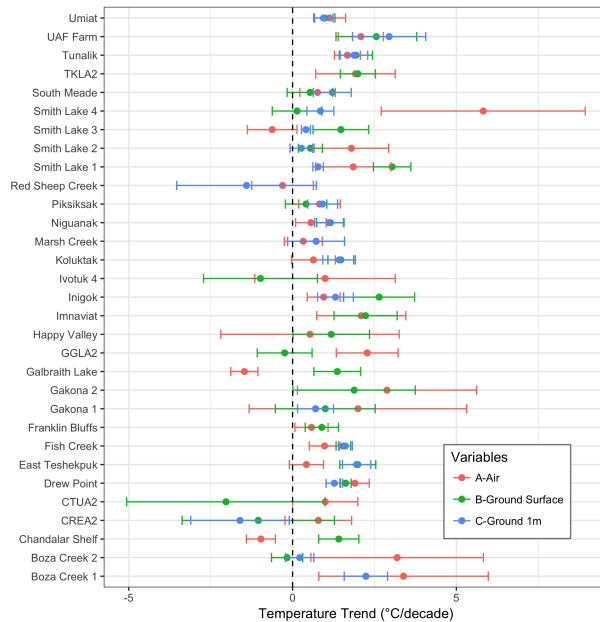


**Figure 7.** Trend comparison of air temperature, ground surface temperature, and ground temperature at 1 m. All trends were estimated only for the stations with  $\geq 5$ -yr available data.

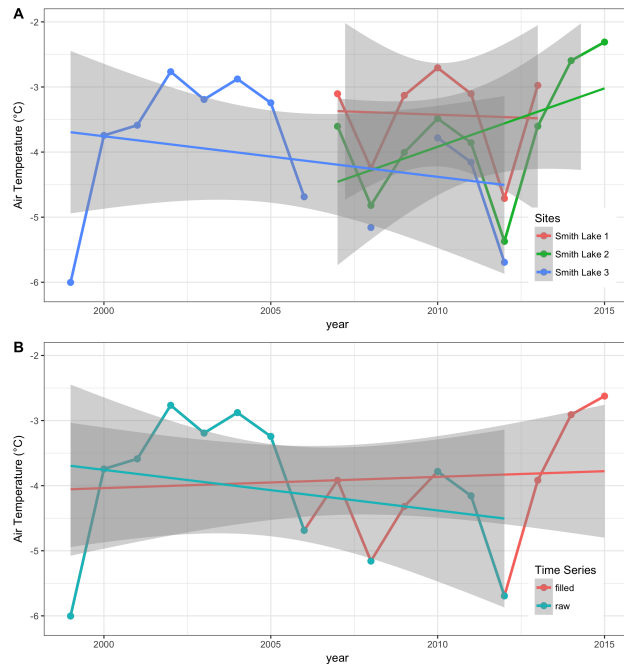


**Figure 8.** Comparison between A) trends calculated using measured data at Smith Lake 1,2, and 3; B) extended data and corrected trends at Smith Lake site 3.

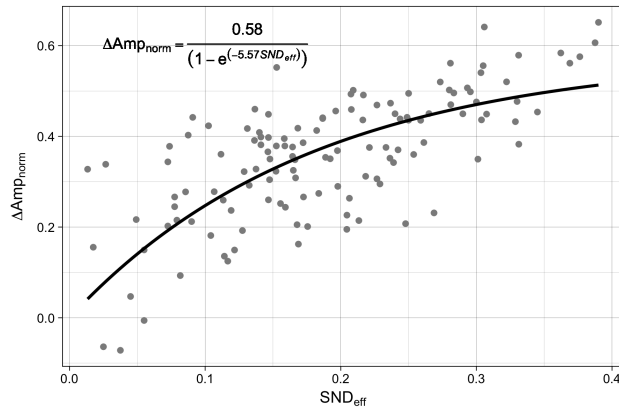


**Figure 9.** Correlation between effective snow depth and normalized temperature amplitude difference between air and ground surface. The mathematical function of fit line was following the correlation showed in Slater et al. (2017).

ground surface temperature) at sites with an effective snow depth over 0.5 m. Over the available observed range (snow depth < 0.4 m), SHTM suggests a positive and roughly linear relationship (Fig.9), implying snow insulation effects increase with increasing effective snow depth, which is consistent with previous studies(Burn and Smith, 1988; Demezhko and Shchapov, 2001; Zhang, 2005; Morse et al., 2012; Slater et al., 2017).

5 In this section, we presented two technical validations that are needed to support the technical quality and information justifying the reliability of these data. This information may help other researchers reuse this dataset.

#### 4 Conclusions

Near-surface ground temperatures are important indicators of the rapidly warming Arctic, because they provide vital information on the response of the ground to climate change. In this paper, we describe the data compilation process listing the 10 work-flow and the challenges associated with preparing our synthesis permafrost dataset for Alaska. Standard unified protocols developed nationally and internationally to monitor near-surface permafrost conditions could significantly improve and simplify the development of corresponding permafrost benchmarks, and reduce the amount of time and effort required for data processing. This dataset consists of 41,667 monthly values during the data collection period (1997-2016). These data were quality-controlled in data collection and data processing stages. We also implemented data harmonization validation for this 15 compiled dataset. The PF-AK v0.1 can be easily integrated into model-data intercomparison tools such as International Land Model Benchmarking (ILAMB) tool (Luo et al., 2012). This dataset should be a valuable permafrost dataset and worth maintaining in the future. Widely, it also provides a prototype of basic data collection and management for remaining permafrost regions.



## 5 Data availability

The latest compiled dataset is available at the Arctic Data Center (<https://doi.org/10.18739/A2KG55>).

*Competing interests.* The authors declare that they have no conflict of interest.

*Acknowledgements.* This study was supported by the National Science Foundation (Award No. 1503559) and the NASA CMAC-14 project (No. NNX16AB19G). GC and FU were supported by the U.S. Geological Survey's Climate and Land Use Change Program. National Park Service data collection is supported by the NPS Inventory and Monitoring Program. GI-UAF Permafrost Lab data collection was supported by the National Science Foundation (Awards OPP-0120736, ARC-0632400, ARC-0520578, ARC-0612533, and ARC-1304271) and by the State of Alaska. TZ was supported by the National Natural Science Foundation of China (Award No. 91325202) and the National Key Scientific Research Program of China (Award No. 2013CBA01802). We thank Dr. David Swanson for insightful comments and suggestions on this manuscript. We also appreciate all for producing and making their data available. Any use of trade, firm, or product names is for descriptive purposes only and does not imply endorsement by the U.S. Government.



## References

- Abbott, B. W., Jones, J. B., Schuur, E. A. G., Chapin, F. S., Bowden, W. B., Bret-Harte, M. S., Epstein, H. E., Flannigan, M. D., Harms, T. K., Hollingsworth, T. N., Mack, M. C., McGuire, A. D., Natali, S. M., Rocha, A. V., Tank, S. E., Turetsky, M. R., Vonk, J. E., Wickland, K. P., Aiken, G. R., Alexander, H. D., Amon, R. M. W., Benscoter, B. W., Bergeron, Y., Bishop, K., Blarquez, O., Bond-Lamberty, B., Breen, A. L., Buffam, I., Cai, Y. H., Carcaillet, C., Carey, S. K., Chen, J. M., Chen, H. Y. H., Christensen, T. R., Cooper, L. W., Cornelissen, J. H. C., de Groot, W. J., DeLuca, T. H., Dorrepaal, E., Fetcher, N., Finlay, J. C., Forbes, B. C., French, N. H. F., Gauthier, S., Girardin, M. P., Goetz, S. J., Goldammer, J. G., Gough, L., Grogan, P., Guo, L. D., Higuera, P. E., Hinzman, L., Hu, F. S., Hugelius, G., Jafarov, E. E., Jandt, R., Johnstone, J. F., Karlsson, J., Kasischke, E. S., Kattner, G., Kelly, R., Keuper, F., Kling, G. W., Kortelainen, P., Kouki, J., Kuhry, P., Laudon, H., Laurion, I., Macdonald, R. W., Mann, P. J., Martikainen, P. J., McClelland, J. W., Molau, U., Oberbauer, S. F., Olefeldt, D., Pare, D., Parisien, M. A., Payette, S., Peng, C. H., Pokrovsky, O. S., Rastetter, E. B., Raymond, P. A., Reynolds, M. K., Rein, G., Reynolds, J. F., Robards, M., Rogers, B. M., Schadel, C., Schaefer, K., Schmidt, I. K., Shvidenko, A., Sky, J., Spencer, R. G. M., Starr, G., Striegl, R. G., Teisserenc, R., Tranvik, L. J., Virtanen, T., Welker, J. M., and Zimov, S.: Biomass offsets little or none of permafrost carbon release from soils, streams, and wildfire: an expert assessment, *Environmental Research Letters*, 11, 34 014–34 014, <https://doi.org/10.1088/1748-9326/11/3/034014>, 2016.
- Bellingham, B. K.: Comprehensive Stevens Hydra Probe Users Manual, Report, 2015.
- Bieniek, P. A., Walsh, J. E., Thoman, R. L., and Bhatt, U. S.: Using Climate Divisions to Analyze Variations and Trends in Alaska Temperature and Precipitation, *Journal of Climate*, 27, 2800–2818, <https://doi.org/10.1175/Jcli-D-13-00342.1>, 2014.
- Box, G., Hunter, J. S., and Hunter, W. G.: *Statistics for experimenters: design, innovation, and discovery*, vol. 2, Wiley-Interscience New York, 2005.
- Brown, J., Ferrians, O., Heginbottom, J. A., and Melnikov, E.: Circum-Arctic Map of Permafrost and Ground-Ice Conditions, Version 2, [http://nsidc.org/data/docs/fgdc/ggd318\\_map\\_circumarctic](http://nsidc.org/data/docs/fgdc/ggd318_map_circumarctic), 1998.
- Brown, J., Hinkel, K. M., and Nelson, F. E.: The circumpolar active layer monitoring (calm) program: Research designs and initial results, *Polar Geography*, 24, 166–258, <https://doi.org/10.1080/10889370009377698>, 2000.
- Burn, C. R. and Smith, C. A. S.: Observations of the Thermal Offset in near-Surface Mean Annual Ground Temperatures at Several Sites near Mayo, Yukon-Territory, Canada, *Arctic*, 41, 99–104, 1988.
- Callaghan, T. V., Tweedie, C. E., Akerman, J., Andrews, C., Bergstedt, J., Butler, M. G., Christensen, T. R., Cooley, D., Dahlberg, U., Danby, R. K., Daniels, F. J., de Molenaar, J. G., Dick, J., Mortensen, C. E., Ebert-May, D., Emanuelsson, U., Eriksson, H., Hedenas, H., Henry, H. R. G., Hik, D. S., Hobbie, J. E., Jantze, E. J., Jaspers, C., Johansson, C., Johansson, M., Johnson, D. R., Johnstone, J. F., Jonasson, C., Kennedy, A. J., Keuper, F., Koh, S., Krebs, C. J., Lantuit, H., Lara, M. J., Lin, D., Lougheed, V. L., Madsen, J., Matveyeva, N., McEwen, D. C., Myers-Smith, I. H., Narozhniy, Y. K., Olsson, H., Pohjola, V. A., Price, L. W., Riget, F., Rundqvist, S., Sandstrom, A., Tamstorf, M., Van Bogaert, R., Villarreal, S., Webber, P. J., and Zemtsov, V. A.: Multi-decadal changes in tundra environments and ecosystems: synthesis of the International Polar Year-Back to the Future project (IPY-BTF), *Ambio*, 40, 705–16, <https://doi.org/10.1007/s13280-011-0179-8>, 2011.
- Demezhko, D. Y. and Shchapov, V. A.: 80,000 years ground surface temperature history inferred from the temperature–depth log measured in the superdeep hole SG-4 (the Urals, Russia), *Global and Planetary Change*, 29, 219–230, [https://doi.org/https://doi.org/10.1016/S0921-8181\(01\)00091-1](https://doi.org/10.1016/S0921-8181(01)00091-1), 2001.



- Hill, K. and Sousanes, P.: Climate station maintenance in the Central Alaska Inventory and Monitoring Network: 2015 summary, Report, 2015.
- Hinzman, L. D., Deal, C. J., McGuire, A. D., Mernild, S. H., Polyakov, I. V., and Walsh, J. E.: Trajectory of the Arctic as an integrated system, *Ecological Applications*, 23, 1837–1868, <https://doi.org/10.1890/11-1498.1>, 2013.
- 5 IPCC: Climate change 2013: the physical science basis. Contribution of Working Group I to the Fifth Assessment Report of the Intergovernmental Panel on Climate Change [Stocker, T.F., D. Qin, G.-K. Plattner, M. Tignor, S.K. Allen, J. Boschung, A. Nauels, Y. Xia, Cambridge University Press, Cambridge, United Kingdom and New York, NY, USA, 2013.
- Jorgenson, M., Yoshikawa, K., Kanevskiy, M., and Shur, Y.: Permafrost characteristics of Alaska, in: Proceedings of the Ninth International Conference on Permafrost, vol. 29, pp. 121–122, 2008.
- 10 Knoblauch, C., Beer, C., Liebner, S., Grigoriev, M. N., and Pfeiffer, E.-M.: Methane production as key to the greenhouse gas budget of thawing permafrost, *Nature Climate Change*, pp. 309–312, <https://doi.org/10.1038/s41558-018-0095-z>, 2018.
- Koven, C. D., Lawrence, D. M., and Riley, W. J.: Permafrost carbon–climate feedback is sensitive to deep soil carbon decomposability but not deep soil nitrogen dynamics, *Proceedings of the National Academy of Sciences*, 112, 3752–3757, <https://doi.org/10.1073/pnas.1415123112>, 2015.
- 15 Liljedahl, A. K., Boike, J., Daanen, R. P., Fedorov, A. N., Frost, G. V., Grosse, G., Hinzman, L. D., Iijima, Y., Jorgenson, J. C., and Matveyeva, N.: Pan-Arctic ice-wedge degradation in warming permafrost and its influence on tundra hydrology, *Nature Geoscience*, 9, 312–318, <https://doi.org/10.1038/ngeo2674>, 2016.
- Luo, Y. Q., Randerson, J. T., Abramowitz, G., Bacour, C., Blyth, E., Carvalhais, N., Ciais, P., Dalmonech, D., Fisher, J. B., Fisher, R., Friedlingstein, P., Hibbard, K., Hoffman, F., Huntzinger, D., Jones, C. D., Koven, C., Lawrence, D., Li, D. J., Mahecha, M., Niu, S. L., 20 Norby, R., Piao, S. L., Qi, X., Peylin, P., Prentice, I. C., Riley, W., Reichstein, M., Schwalm, C., Wang, Y. P., Xia, J. Y., Zaehle, S., and Zhou, X. H.: A framework for benchmarking land models, *Biogeosciences*, 9, 3857–3874, <https://doi.org/10.5194/bg-9-3857-2012>, 2012.
- McGuire, A. D., Koven, C., Lawrence, D. M., Clein, J. S., Xia, J., Beer, C., Burke, E., Chen, G., Chen, X., Delire, C., Jafarov, E., MacDougall, A. H., Marchenko, S., Nicolsky, D., Peng, S., Rinke, A., Saito, K., Zhang, W., Alkama, R., Bohn, T. J., Ciais, P., Decharme, B., Ekici, A., Gouttevin, I., Hajima, T., Hayes, D. J., Ji, D., Krinner, G., Lettenmaier, D. P., Luo, Y., Miller, P. A., Moore, J. C., Romanovsky, V., Schädel, C., Schaefer, K., Schuur, E. A. G., Smith, B., Sueyoshi, T., and Zhuang, Q.: Variability in the sensitivity among model simulations of permafrost and carbon dynamics in the permafrost region between 1960 and 2009, *Global Biogeochemical Cycles*, 30, 1015–1037, <https://doi.org/10.1002/2016GB005405>, 2016.
- Melvin, A. M., Larsen, P., Boehlert, B., Neumann, J. E., Chinowsky, P., Espinet, X., Martinich, J., Baumann, M. S., Rennels, L., Bothner, A., Nicolsky, D. J., and Marchenko, S. S.: Climate change damages to Alaska public infrastructure and the economics of proactive adaptation, 30 Proceedings of the National Academy of Sciences, 114, E122–E131, <https://doi.org/10.1073/pnas.1611056113>, 2017.
- Menne, M. J., Williams, C. N., and Vose, R. S.: The U.S. Historical Climatology Network Monthly Temperature Data, Version 2, *Bulletin of the American Meteorological Society*, 90, 993–1007, <https://doi.org/10.1175/2008bams2613.1>, 2009.
- Morse, P. D., Burn, C. R., and Kokelj, S. V.: Influence of snow on near-surface ground temperatures in upland and alluvial environments of the outer Mackenzie Delta, Northwest Territories, *Canadian Journal of Earth Sciences*, 49, 895–913, <https://doi.org/10.1139/E2012-012>, 35 2012.
- Nelson, F. E. and Outcalt, S. I.: A computational method for prediction and regionalization of permafrost, *Arctic and Alpine Research*, pp. 279–288, 1987.



Plummer, N., Allsopp, T., Lopez, J. A., and Llansó, P.: Guidelines on Climate Observation: Networks and Systems, World Meteorological Organization, 2003.

Romanovsky, V., Marchenko, S., Daanen, R., Sergeev, D., and Walker, D.: Soil climate and frost heave along the permafrost/ecological North American Arctic transect, in: Proceedings of the Ninth International Conference on Permafrost, vol. 2, pp. 1519–1524, Institute of 5 Northern Engineering: Fairbanks, AK, 2008.

Romanovsky, V., Cable, W., and Kholodov, A.: Changes in permafrost and active-layer temperatures along an Alaskan permafrost-ecological transect, in: Proc. 68th Canadian Geotechnical Conf. and Seventh Canadian Conf. on Permafrost (GEOQuébec 2015), 2015.

Schaefer, K., Lantuit, H., Romanovsky, V. E., Schuur, E. A. G., and Witt, R.: The impact of the permafrost carbon feedback on global climate, Environmental Research Letters, 9, 85 003–85 003, <https://doi.org/10.1088/1748-9326/9/8/085003>, 2014.

10 Sherstiukov, A.: Dataset of daily soil temperature up to 320 cm depth based on meteorological stations of Russian Federation, RIHMI-WDC, 176, 224–232, 2012.

Shiklomanov, N., Nelson, F., Streletskiy, D., Hinkel, K., and Brown, J.: The circumpolar active layer monitoring (CALM) program: data collection, management, and dissemination strategies, in: Proceedings of the ninth international conference on permafrost, vol. 29, Institute of Northern Engineering Fairbanks, Alaska, 2008.

15 Shiklomanov, N. I., Streletskiy, D. A., Swales, T. B., and Kokorev, V. A.: Climate Change and Stability of Urban Infrastructure in Russian Permafrost Regions: Prognostic Assessment Based on Gcm Climate Projections, Geographical Review, 107, 125–142, <https://doi.org/10.1111/gere.12214>, 2017.

Slater, A. G., Lawrence, D. M., and Koven, C. D.: Process-level model evaluation: a snow and heat transfer metric, Cryosphere, 11, 989–996, <https://doi.org/10.5194/tc-11-989-2017>, 2017.

20 Urban, F. E. and Clow, G. D.: DOI/GTN-P Climate and active-layer data acquired in the National Petroleum Reserve–Alaska and the Arctic National Wildlife Refuge, 1998–2015, Report 1021, <https://doi.org/10.3133/ds1021>, 2017.

Wang, K., Zhang, T., and Zhong, X.: Changes in the timing and duration of the near surface soil freeze/thaw status from 1956 to 2006 across China, Cryosphere, 9, 1321–1331, <https://doi.org/10.5194/tc-9-1321-2015>, 2015.

25 Wang, K., Zhang, T. J., Zhang, X. D., Clow, G. D., Jafarov, E. E., Overeem, I., Romanovsky, V., Peng, X. Q., and Cao, B.: Continuously amplified warming in the Alaskan Arctic: Implications for estimating global warming hiatus, Geophysical Research Letters, 44, 9029–9038, <https://doi.org/10.1002/2017gl074232>, 2017.

Yershov, E. D. and Williams, P. J.: General geocryology, Cambridge university press, 2004.

Zhang, T., Barry, R. G., Knowles, K., Heginbottom, J. A., and Brown, J.: Statistics and characteristics of permafrost and ground-ice distribution in the Northern Hemisphere, Polar Geography, 23, 132–154, <https://doi.org/10.1080/10889379909377670>, 1999.

30 Zhang, T. J.: Influence of the seasonal snow cover on the ground thermal regime: An overview, Reviews of Geophysics, 43, <https://doi.org/10.1029/2004rg000157>, 2005.



**Table 1.** Overview of the data from the permafrost monitoring stations in Alaska

Name	Latitude	Longitude	Onset	Last	MAAT	MAGST	MAGT 1 m	Snow Depth	Source	Number of available annual statistics							Number of available annual statistics		
										Name	Latitude	Longitude	Onset	Last	MAAT	MAGST	MAGT 1 m	Snow Depth	Source
Avunai	69.17	-158.01	1998	2004	3	2	2	1	USGS	Smith Lake 1	64.87	-147.86	1997	2016	9	9	9	9	GI-UAF
Avunai2	69.16	-158.03	2003	2015	7	1	1	5	USGS	Smith Lake 2	64.87	-147.86	2006	2016	9	7	9	9	GI-UAF
Candus Bay	69.97	-144.77	2003	2015	7	1	1	1	USGS	Smith Lake 3	64.87	-147.86	1997	2016	4	5	8	8	GI-UAF
Drew Point	70.86	-153.91	1998	2015	11	12	12	8	USGS	Smith Lake 4	64.87	-147.86	2006	2016	7	7	7	7	GI-UAF
East Teshekpuk	70.57	-152.97	2004	2015	1	1	1	1	USGS	UAF Farm	64.85	-147.86	2007	2016	7	6	5	4	GI-UAF
Fish Creek	70.34	-152.05	1998	2015	14	15	15	11	USGS	West Dock	70.37	-148.55	2001	2016	9	4	3	3	GI-UAF
Ipihukpuk	70.44	-154.37	2005	2015	9	4	5	5	USGS	Gakona 1	62.39	-145.15	2009	2016	5	5	5	5	GI-UAF
Inigok	69.99	-153.09	1998	2015	12	7	1	14	USGS	Gakona 2	62.39	-145.15	2009	2016	5	5	3	3	GI-UAF
Koluktaik	69.75	-154.62	1999	2015	9	6	11	1	USGS	ASIA2	67.47	-162.27	2012	2016	3	2	2	2	NPS
Lake 45 Shore	70.69	-152.63	2007	2015	4	5	5	5	USGS	CCLA2	65.31	-143.13	2004	2016	11	8	8	8	NPS
Marsh Creek	69.78	-144.79	2001	2015	12	1	7	12	USGS	CHMA2	67.71	-150.59	2012	2016	3	2	2	2	NPS
Niguanak	69.89	-142.98	2000	2015	14	14	14	11	USGS	CRIA2	62.12	-141.85	2004	2016	11	5	5	5	NPS
Pihsikuk	70.04	-157.08	2004	2015	1	7	1	8	USGS	CTUA2	61.27	-142.62	2004	2016	11	5	9	9	NPS
Red Sheep Creek	68.68	-144.84	2004	2015	7	1	6	7	USGS	DKLA2	63.27	-149.54	2004	2016	9	4	7	7	NPS
South Meade	70.63	-156.84	2003	2015	1	8	1	8	USGS	DVLA2	66.28	-164.53	2011	2016	4	1	1	1	NPS
Tunulik	70.20	-161.08	1998	2015	13	8	14	13	USGS	ELIA2	65.28	-163.82	2012	2016	3	1	1	1	NPS
Umiat	69.40	-152.14	1998	2015	14	13	13	11	USGS	GGLA2	61.60	-143.01	2005	2016	1	5	5	5	NPS
Barrow 2	71.31	-156.66	2002	2016	4	9	6	4	GI-UAF	HOWA2	68.16	-156.90	2011	2016	3	1	1	1	NPS
Boza Creek 1	64.71	-148.29	2009	2016	6	1	6	5	GI-UAF	IMYA2	67.54	-157.08	2012	2016	3	1	1	1	NPS
Boza Creek 2	64.72	-148.29	2009	2016	6	6	6	6	GI-UAF	KAU2	67.57	-158.43	2012	2016	3	1	1	1	NPS
Chandalar Shelf	68.07	-149.58	1997	2016	11	11	11	11	GI-UAF	KLIA2	67.98	-155.01	2012	2016	2	1	1	1	NPS
Deadhorse	70.16	-148.47	1997	2016	3	3	3	3	GI-UAF	KUGA2	68.32	-161.49	2014	2016	1	1	1	1	NPS
Fox	64.95	-147.62	2001	2016	3	6	6	4	GI-UAF	MITA2	65.82	-164.54	2011	2016	3	1	1	1	NPS
Franklin Bluffs	69.67	-148.72	1997	2016	13	1	6	5	GI-UAF	MNOA2	67.14	-162.99	2011	2016	4	1	1	1	NPS
Franklin Bluffs boil	69.67	-148.72	2007	2016	4	6	6	6	GI-UAF	PAMA2	67.77	-152.16	2012	2016	2	2	2	2	NPS
Franklin Bluffs interior boil	69.67	-148.72	2006	2016	6	6	6	6	GI-UAF	RAMA2	67.62	-154.34	2012	2016	1	1	1	1	NPS
Franklin Bluffs' We	69.68	-148.72	2006	2016	3	3	3	3	GI-UAF	RUGA2	62.71	-150.54	2008	2016	4	2	2	2	NPS
Galbraith Lake	68.48	-149.50	2001	2016	6	6	6	6	GI-UAF	SRTA2	65.85	-164.71	2011	2016	4	3	3	3	NPS
Happy Valley	69.16	-148.84	2001	2016	6	8	8	4	GI-UAF	SRWA2	67.46	-159.84	2011	2016	1	2	2	2	NPS
Imaviat	68.64	-149.35	2006	2016	8	8	8	8	GI-UAF	SSIA2	68.00	-160.40	2011	2016	4	2	2	2	NPS
Ivouk 3	68.48	-155.74	2006	2013	2	2	2	2	GI-UAF	TAHA2	67.55	-163.57	2011	2016	3	3	3	3	NPS
Ivouk 4	68.48	-155.74	1998	2016	6	5	1	6	GI-UAF	TANA2	60.91	-142.90	2005	2016	5	3	3	3	NPS
Pilgrim Hot Springs	65.99	-164.90	2012	2016	2	2	2	3	GI-UAF	TEBA2	61.18	-144.34	2005	2016	8	6	6	6	NPS
Sag! MNT	69.43	-148.67	2001	2016	7	3	1	1	GI-UAF	TKLA2	63.52	-150.04	2005	2016	1	1	1	1	NPS
Saq2 MAT	69.43	-148.70	2001	2016	11	3	3	3	GI-UAF	UPRA2	64.52	-143.20	2005	2016	9	3	4	4	NPS
Selawik Village	66.61	-160.02	2012	2016	3	3	3	3	GI-UAF	WIGA2	63.81	-150.11	2013	2016	2	1	1	1	NPS



**Table 2.** Summary of the air, ground surface, ground temperature at 1 m, volumetric water content and snow depth over the entire observation period.

Site	Air Temperature (°C)			Ground Surface Temperature (°C)			Ground Temperature at 1 m (°C)			VWC (m³/m³)			Snow Depth (m)	
	Min	Mean	Max	Min	Mean	Max	Min	Mean	Max	Min	Mean	Max	Mean	Max
Awuna1	-28.51	-10.61	9.62	-11.30	-4.16	2.79	-9.38	-4.52	-0.93				0.39	0.61
Awuna2	-30.47	-9.88	11.60	-13.21	-3.34	8.10	-10.84	-4.43	-0.64	0.02	0.21	0.43	0.37	0.54
Camden Bay	-28.89	-10.35	6.92				-14.47	-7.49	-1.20				0.20	0.26
Drew Point	-28.62	-10.84	6.04	-20.60	-7.63	4.74	-16.02	-7.84	-1.68				0.18	0.29
East Teshekpuk	-28.19	-10.27	7.79	-17.97	-6.26	4.07	-14.20	-6.91	-1.90	0.01	0.18	0.42	0.23	0.32
Fish Creek	-29.07	-10.55	8.81	-16.85	-6.02	4.50	-14.11	-6.82	-1.17	0.01	0.17	0.41	0.20	0.28
Ikpikpuk	-29.15	-10.27	9.21	-18.08	-5.49	5.60							0.22	0.37
Inigok	-29.98	-10.58	10.55	-16.28	-4.80	7.73	-12.68	-5.58	-0.60	0.00	0.12	0.33	0.22	0.33
Koluktak	-30.02	-10.18	11.64	-15.20	-3.77	8.75	-13.77	-4.69	1.16	0.02	0.13	0.36	0.20	0.30
Lake145Shore	-28.72	-10.50	7.30							0.06	0.21	0.41	0.28	0.42
Marsh Creek	-26.51	-8.65	10.20	-16.87	-5.28	5.26	-14.39	-6.11	-0.82	0.03	0.16	0.41	0.19	0.25
Niguanak	-27.80	-9.97	8.48	-18.13	-6.09	4.66	-14.87	-6.72	-1.02				0.15	0.21
Piksiksak	-29.21	-9.93	10.71	-17.65	-5.76	6.21	-13.44	-5.94	-0.87				0.10	0.16
Red Sheep Creek	-23.94	-6.81	12.88	-10.04	-2.76	8.84	-8.78	-3.56	-0.36	0.02	0.25	0.74	0.23	0.38
South Meade	-29.90	-10.42	9.35	-19.91	-6.45	5.89	-15.74	-7.19	-1.12				0.19	0.29
Tunalik	-28.26	-10.17	9.15	-21.58	-7.12	6.81	-16.18	-7.35	-0.92				0.17	0.28
Umiat	-28.67	-9.84	11.18	-14.24	-4.66	4.71	-10.96	-5.14	-1.04				0.32	0.44
Barrow 2	-26.55	-10.23	5.09	-19.17	-6.87	5.33	-15.46	-7.41	-1.59	0.02	0.16	0.39	0.14	0.22
Boza Creek 1	-25.00	-3.20	16.03	-9.17	1.13	12.93	-4.58	-1.27	-0.29	0.00	0.20	0.55	0.18	0.36
Boza Creek 2	-23.60	-2.18	16.31	-3.62	2.28	12.00	-0.46	0.09	1.23	0.06	0.22	0.40		
Chandalar Shelf	-23.66	-7.64	11.41	-9.54	-1.29	7.74				0.00	0.22	0.74		
Deadhorse	-28.04	-9.97	8.27	-14.89	-3.65	7.13				0.03	0.16	0.38		
Fox	-26.02	-2.99	16.03							0.08	0.24	0.40		
Franklin Bluffs	-30.15	-10.62	10.74	-14.65	-3.89	8.38				0.02	0.19	0.47		
Franklin Bluffs boil				-18.04	-4.15	11.99								
Franklin Bluffs interior boil				-16.85	-3.66	11.12								
Franklin Bluffs Wet	-28.56	-10.49	10.84	-14.52	-3.36	10.28								
Galbraith Lake	-28.77	-9.35	10.72	-14.38	-3.45	9.34								
Happy Valley	-30.01	-9.49	12.30	-9.31	-1.63	7.19				0.02	0.14	0.31	0.27	0.47
Imnaviat	-22.95	-6.81	10.57	-8.48	-0.81	8.54								
Ivotuk 3	-29.85	-10.12	11.30	-9.97	-1.14	6.99								
Ivotuk 4	-29.10	-9.70	11.23	-9.21	-1.24	8.26	-5.16	-1.89	-0.53	0.00	0.27	0.77	0.43	0.60
Pilgrim Hot Springs	-16.78	-2.04	14.63	-11.95	0.08	13.52	-7.56	-2.30	-0.27	0.00	0.30	0.73	0.06	0.21
Sag1 MNT	-26.72	-8.39	10.68	-17.14	-4.27	9.48	-13.50	-5.00	0.24	0.04	0.20	0.40		
Sag2 MAT				-15.11	-3.76	9.01	-11.03	-4.49	-0.45	0.02	0.26	0.63		
Selawik Village	-20.26	-3.72	14.91	-11.16	-0.74	12.18	-7.99	-3.09	-0.45				0.05	0.12



**Table 2.** Summary of the air, ground surface, ground temperature at 1 m, volumetric water content and snow depth over the entire observation period—continued.

Site	Air Temperature (°C)			Ground Surface Temperature (°C)			Ground Temperature at 1 m (°C)			VWC (m <sup>3</sup> /m <sup>3</sup> )			Snow Depth (m)	
	Min	Mean	Max	Min	Mean	Max	Min	Mean	Max	Min	Mean	Max	Mean	Max
Smith Lake 1	-23.88	-3.06	16.06	-11.29	-0.11	12.98	-2.02	-0.73	-0.26	0.02	0.14	0.31		
Smith Lake 2	-24.91	-3.74	15.98	-7.32	1.10	12.86	-4.10	-1.11	0.00	0.07	0.29	0.59		
Smith Lake 3	-27.29	-4.70	14.68	-3.49	2.57	11.51	-0.33	0.00	0.88	0.07	0.23	0.40		
Smith Lake 4	-26.15	-3.58	18.20	-15.81	-2.27	9.68	-10.32	-3.81	-0.62					
UAF Farm	-22.09	-1.48	16.57	-10.91	0.68	13.00	-0.83	1.18	5.43				0.28	0.47
West Dock	-28.82	-10.53	6.81	-20.30	-6.68	5.46				0.01	0.20	0.55	0.04	0.09
Gakona 1	-23.06	-2.76	13.70	-5.29	1.55	11.26	-1.62	-0.63	-0.22					
Gakona 2	-23.01	-2.45	14.00	-5.54	1.35	9.63	-0.72	-0.18	0.75					
ASIA2	-15.10	-3.20	12.24										0.02	0.07
CCLA2	-27.39	-4.52	15.90										0.33	0.52
CHMA2	-15.97	-5.24	9.81										0.04	0.08
CREA2	-16.41	-3.87	8.57	-12.35	-1.78	11.22	-6.00	-2.13	0.35				0.12	0.21
CTUA2	-14.15	-2.52	8.61	-12.83	-1.09	12.43							0.08	0.16
DKLA2	-17.19	-3.32	10.72				-3.33	1.22	7.03				0.39	0.64
DVLA2	-21.84	-5.38	10.77											
ELLA2	-17.18	-4.81	9.93										0.29	0.43
GGLA2	-13.51	-2.01	9.13	-1.50	2.54	12.18							0.90	1.45
HOWA2	-23.29	-6.64	10.18										0.05	0.11
IMYA2	-15.30	-5.19	8.96										0.15	0.26
KAU2	-21.65	-6.47	10.01										0.15	0.25
KLIA2	-19.10	-7.66	7.38										0.07	0.10
KUGA2	-16.74	-3.56	13.64										0.18	0.59
MITA2														
MNOA2	-18.78	-3.79	12.47										0.14	0.37
PAMA2	-18.00	-4.49	11.02										0.07	0.11
RAMA2	-17.93	-5.42	10.77											
RUGA2	-9.49	-0.53	10.45										0.50	0.83
SRTA2	-21.96	-4.69	11.77										0.06	0.16
SRWA2	-17.35	-3.15	13.89										0.34	0.68
SSIA2	-21.85	-5.86	11.27										0.02	0.06
TAHA2	-20.09	-4.48	11.58										0.09	0.20
TANA2	-13.83	-2.02	9.91										1.01	1.55
TEBA2	-17.27	-1.92	11.54										0.75	1.34
TKLA2	-18.48	-3.15	11.39	-6.93	1.63	13.17							0.15	0.25
UPRA2	-21.39	-4.91	11.36	-13.19	-1.69	12.80							0.33	0.48
WIGA2	-17.84	-1.55	13.21										0.10	0.15



**Table 3.** Summary of the freezing (DDF) and thawing index (DDT) of air and ground temperatures over the entire observation period (unit:  $^{\circ}\text{C} - \text{day}$ ).

Site	Air		Ground Surface		Ground 0.25 m		Ground 0.50 m		Ground 0.75 m		Ground 1.00 m	
	DDF	DDT	DDF	DDT	DDF	DDT	DDF	DDT	DDF	DDT	DDF	DDT
Awuna1	4217	769	1750	196	1862	10	1878	0	1880	0	1880	0
Awuna2	4417	975	1740	807	1939	233	2086	7	2121	0	2095	0
Camden Bay	4493	482			2684	100	2858	0	2873	0	2860	0
Drew Point	4521	400	3221	327	3291	46	3280	0	3248	0	3231	0
East Teshekpuk	4298	576	2815	279	2964	18	2982	0	2951	0	2939	0
Fish Creek	4376	677	2582	328	2813	12	2821	0	2804	0	2789	0
Ikpikpuk	4356	718	2712	434	2685	225						
Inigok	4404	858	2268	708	2454	60	2491	0	2449	0	2423	0
Koluktak	4337	984	2034	856	2242	618	2309	325	2340	153	2355	54
Lake145Shore	4430	522										
Marsh Creek	3836	860	2526	408	2831	159	2863	20	2801	0	2776	0
Niguanak	4179	654	2798	339	2952	54	2960	1	2934	0	2900	0
Piksiksak	4263	886	2594	506	2700	66	2707	0	2657	0	2611	0
Red Sheep Creek	3249	1230	1208	989	1637	324	1715	58	1710	0	1667	0
South Meade	4477	727	3006	447	3186	45	3214	0	3187	0	3078	0
Tunalik	4213	725	3230	535	3258	138	3225	8	3160	0	3120	0
Umiat	4138	948	2114	374	2306	14	2271	0	2216	0	2189	0
Barrow 2	4241	325	2925	398	2996	85	3072	0	3049	0	3112	0
Boza Creek 1	3270	1634	959	1646	676	581	832	81	917	1	888	0
Boza Creek 2	3036	1704	278	1808	224	839	166	550	103	308	47	188
Chandalar Shelf	3285	1049	1184	855	1352	55	1302	0	1388	0		
Deadhorse	4236	628	2070	654	2106	261	2144	101	2236	3		
Fox	3441	1618			192	442	214	21	191	0		
Franklin Bluffs	4420	879	1964	820	2096	237	2114	61	2289	1		
Franklin Bluffs boil			2339	1234	2293	792	2117	414	2018	193		
Franklin Bluffs interior boil			2192	1145	2132	498	2166	288	2073	111		
Franklin Bluffs Wet	4142	907	1873	1100	1733	635	1734	689	1702	68		
Galbraith Lake	4190	895	1875	955	2050	167	2110	14	2123	0		
Happy Valley	4293	1061	1167	781	1245	211	1337	36	1404	0		
Imnaviat	3212	954	994	1005	1017	460	1053	218	1086	93		
Ivotuk 3	4332	948	1273	729	1134	127	1312	3	1312	0		
Ivotuk 4	4209	948	1105	933	1142	579	1248	120	1290	6	1038	0
Pilgrim Hot Springs	2025	1632	1346	1631	1723	168	1583	18	1465	1	1427	0
Sag1 MNT	3840	912	2313	914	2209	521	2227	202	2259	36	2425	5
Sag2 MAT			2012	900	2207	186	2287	44	2281	12	2098	3
Selawik Village	2556	1579	1266	1452	1626	148	1695	0	1608	0	1542	0



**Table 3.** Summary of the freezing and thawing index of air and ground temperatures over the entire observation period (unit:  $^{\circ}\text{C} - \text{day}$ )—continued.

Site	Air		Ground Surface		Ground 0.25 m		Ground 0.50 m		Ground 0.75 m		Ground 1.00 m	
	DDF	DDT	DDF	DDT	DDF	DDT	DDF	DDT	DDF	DDT	DDF	DDT
Smith Lake 1	3086	1659	1273	1581	488	70	469	1	429	0	415	0
Smith Lake 2	3254	1624	712	1723	779	392	810	120	781	13	748	1
Smith Lake 3	3703	1403	275	1739	227	773	114	514	60	324	36	137
Smith Lake 4	3384	1934	2084	966	1815	353	2064	39	2082	0	1996	0
UAF Farm	2779	1773	1216	1599	499	1043	279	959	135	949	51	891
West Dock	4491	475	3108	400	3181	22	3186	0	3121	0		
Gakona 1	3068	1361	483	1573	434	303	443	35	437	0	336	0
Gakona 2	3046	1402	564	1311	428	578	261	294	160	233	139	145
ASIA2	1861	1339			1657	1150	1617	1030				
CCLA2	3656	1559			1430	551	1162	23	1113	3		
CHMA2	2104	981			2222	936	1837	478	1537	358		
CREA2	2248	817	1481	1274	1412	725	1267	396	1131	129	1046	15
CTUA2	1880	868	1510	1438	1434	870	1310	751				
DKLA2	2264	1084			725	1350	566	1216	428	1098	321	997
DVLA2	3031	1010			1742	360	1724	143				
ELLA2	2298	975			1545	1030	1530	760				
GGLA2	1753	953	79	2028	17	1824	4	1642				
HOWA2	3292	901			3295	678	3111	516				
IMYA2	2038	880			1849	995	1887	547				
KAUA2	3027	904			1764	623	1674	452				
KLIA2	2763	624			2201	366	2257	208				
KUGA2	2057	1491			1255	1418	1245	1066				
MITA2												
MNOA2	2447	1295			963	1050	1144	959	1059	704		
PAMA2	2374	1101			2135	611	2117	409				
RAMA2	2373	1066			1916	952	1854	1036				
RUGA2	1075	1250										
SRTA2	2998	1138			1192	1147	1063	1122				
SRWA2	2142	1510			928	1826	786	1516				
SSIA2	2993	1062			2234	771	2165	608	1789	526		
TAHA2	2702	1149			1590	1175	1565	1027	1399	631		
TANA2	1770	1053			171	1850	106	1505				
TEBA2	2237	1191			66	1985	28	1757				
TKLA2	2446	1151	669	1809								
UPRA2	2913	1083	1552	1481	1084	1142	884	832				
WIGA2	2246	1402			1053	289	1120	59				